Forest Ecology and Management 399 (2017) 166–178

Contents lists available at ScienceDirect

Forest Ecology and Management

journal homepage: www.elsevier.com/locate/foreco

Analysis and out-year forecast of beetle, borer, and drought-induced tree mortality in California

Haiganoush K. Preisler [a,*], Nancy E. Grulke [b], Zachary Heath [c], Sheri L. Smith [d]

[a] USDA, Forest Service, Pacific South West Research Station, 800 Buchanan St., Albany, CA 94710, USA
[b] USDA, Forest Service, Western Wildland Environmental Threat Assessment Center, 3160 NE 3rdSt., Prineville, OR 97754, USA
[c] USDA, Forest Service, State and Private Forestry, 16400 Champion Way, Sandy, OR 97055, USA
[d] USDA, Forest Service, State and Private Forestry, 2550 Riverside Dr., Susanville, CA 96130, USA

ARTICLE INFO

Article history:
Received 24 March 2017
Received in revised form 11 May 2017
Accepted 22 May 2017
Available online 29 May 2017

Keywords:
Bark beetle outbreak
Drought
Fuels reduction
Forest planning
Generalized additive models
Predictive tool

ABSTRACT

The level of tree mortality and drought observed over the past decade in North America has been described as 'unparalleled' in our modern history, in particular in the Sierra Nevada, California. Forest managers could use early warning of where and how much tree mortality to expect in the very near future to plan and prioritize hazard tree removal, pest suppression activities, infer location of funding needs and fuels reduction treatments as well as access for firefighting. To answer these needs, we developed an empirically-based forecast model for expected tree mortality for an upcoming year based on (1) previous years' tree mortality as observed in late summer; (2) previous years' hydrologic year precipitation levels; and (3) site characteristics including amount of available host. Using this approach, initial forecasts for the next growing season can be developed by late fall for the following late summer. We demonstrated the application of this model by developing a forecast for the state of California for 2017. The explanatory variables in the California model accounted for ~43% of the variability in tree mortality. Overall, the model missed forecasting high levels of mortality in approximately 5% of forested or woodland locations for the state of California. Locations with more mortality than expected in 2015 & 2016 were mostly associated with new outbreaks of insects; land use changes, and margins of prescribed- or wildfires not initially attributed. The forecasts may also be useful to natural resource and land managers in locating new outbreaks that may be attributed to novel behavior or exotic insects.
Published by Elsevier B.V.

1. Introduction

Bark beetle and other insect outbreaks have been common, temporally syncopated, and regionally extensive over the last century as recorded by forest entomologists (Grulke et al., 2009). However, larger-than-expected outbreaks with high tree mortality have appeared globally in the late 20th century and into the 21st century (Allen et al., 2010). Extensive tree mortality has been associated with greater wildfire risk (Hicke et al., 2012).

Among bark beetles and wood borers, higher than average winter minimum temperatures, longer summers with higher average temperatures, and drought are correlated with bark beetle outbreaks (Régnière et al., 2012). Higher winter temperatures, and longer growing seasons are expected to become increasingly common into the future (IPCC, 2014): these may act as antecedent drivers and intensifiers of insect population growth in some cases. Drought-induced tree mortality may also intensify, but its location, severity, frequency, and longevity in an upcoming year is more difficult to accurately predict. Multiple-year droughts can significantly increase the level of tree mortality due to accelerated increase in bark beetle populations (Buotte et al., 2016; Preisler et al., 2012; Grulke et al., 2009).

Although empirical data on inciting factors of outbreaks are available for model parameterization (Bentz et al., 2010 and references within), relatively few insect species have been adequately characterized. Empirical relationships between environmental drivers and insect demographics are needed to parameterize dynamic vegetation models, which translate analog changes in environment into changes in vegetation assemblages through the end of the century. Analog vegetation models (in contrast to state-and-transition vegetation models) permit modeling well into the future, and at the landscape level. Others (Young et al., 2017; Seidl et al., 2015) have identified attributes to explain tree mortality at the landscape level, but not to forecast mortality (within- year, and following

* Corresponding author.
E-mail addresses: hpreisler@fs.fed.us (H.K. Preisler), ngrulke@fs.fed.us (N.E. Grulke), zheath@fs.fed.us (Z. Heath), ssmith11@fs.fed.us (S.L. Smith).

http://dx.doi.org/10.1016/j.foreco.2017.05.039
0378-1127/Published by Elsevier B.V.

year). The most extensive collection of insect responses to the environment and demographic consequences has been developed by entomologists of the USFS Forest Health Protection program (and academics), and assembled by the USFS Forest Health Assessment and Applied Sciences Team (FHAAST, previously known as FHTET; Krist et al., 2010). However, the current level of insect outbreaks and tree mortality observed in British Columbia (Cudmore et al., 2010), in the northern Rocky Mountains (Meddens and Hicke, 2014), and in the Sierra Nevada, CA (Young et al., 2017) are outside the range of values observed at these locations in the recent past. Furthermore, wood or fir borers, often thought to be secondary invaders, can be primary causes of tree mortality (California Forest Pest Council, 2016; flat headed fir borer in Douglas fir, Bill Schaup, pers. comm.; and California flat-headed borer in Jeffrey pine, Nancy Grulke, pers. obs.). There is no, or little, empirical data with which to develop demographic models for the wood borers, as well as other insects with a similar potential in the future. These data take decades to collect. Demographics of yet-to-invade exotic species are particularly difficult to anticipate, yet potential functional types are being identified and anticipated by the Animal and Plant Health Inspection Service (APHIS) and others.

High levels of tree mortality may increase the probability for severe wildfires depending on when fire initiation occurs, relative to dead needle and fine branch retention (Hicke et al., 2012). Forest managers could use forecasts of tree mortality for the following year (current year +1) to anticipate and prioritize hazard tree removal, pest suppression activities, infer location of funding needs and fuels reduction activities and firefighter access to high risk locations.

The concern of the present study is to develop statistical forecasts of combined bark beetle, wood borer, or drought attributed tree mortality (hence forth referred to as BB-WB-D mortality) using prior years observations of the levels and locations of mortalities, availability of host, and environmental conditions known to be inciting factors for that insect guild. The intent of the present work was not to find the best drivers of successful insect attacks, but simply to best forecast the following year location and expected magnitude and range of tree mortality. Only variables that were and are available at least one year ahead of the forecast were used in the forecast models. Given the extreme skewness of the distribution of the variable of concern (number of trees killed per pixel), the level of uncertainty in our forecasts were based on empirical distributions of the data and, consequently, avoid the need for making parametric distributional assumptions.

2. Methods

2.1. Data

Aerial Detection Survey data (ADS) in USDA Forest Service Region 5 (California) and adjacent areas of Region 4 (western Nevada) from the 1993 to 2016 surveys were aggregated to 2.5 min cells (cells roughly four km in width or 1800 hectares in area). ADS collects data on tree mortality using aircraft flying approximately 150–450 m in altitude (Young et al., 2017). Information collected annually includes location, number of affected trees or number of trees per hectare (from 2004 to 2016 only), the likely damage agent, and host tree species. This data was collected on paper maps prior to 2001, and on a georeferenced moving map display on a tablet computer starting in 2001. For this analysis, total hectares with BB-WB-D mortality (regardless of intensity of mortality), were calculated from 1993 to 2016 for each cell, and the total number of trees killed by BB-WB-D, were calculated from 2004 to 2016 for each cell. Cells that were not flown in a given year were assigned a missing value for that year.

Variables pertaining to site characteristics, in addition to those pertaining to weather and 'beetle pressure' are listed in Table 1. Because beetle pressure was not observed directly, we used number of trees killed, or alternatively, area affected with mortality, as a surrogate for beetle pressure. The number of hectares with tree hosts were derived from tree species distribution layers developed by FHAAST (Krist et al., 2010). The datasets were modeled from ground plot data measured by Forest Inventory and Analysis (FIA, Gillespie, 1999) and from predictor datasets consisting of climate, terrain, soils, and satellite imagery (Ellenwood et al., 2015). Area containing host (pooled, regardless of tree species, stand density or basal area) that were affected by BB-WB-D were calculated for each cell. Host tree distributions included ponderosa, Jeffrey, Coulter, Bishop, Monterey, knobcone, sugar, lodgepole, western white, whitebark, limber and pinyon pines; white, grand, red and subalpine fir; and Douglas-fir and big cone Douglas-fir. Area affected by fire in each cell was obtained from CalFire (Table 1). As an estimate of amount of host remaining we used the variable, number of hectares with host minus number of hectares with mortality previous year.

Table 1
List of variables used in predictive models. All variables are at the 2.5′ (1800 ha) grid level.

Variable related to	Units	Source	Description
Site characteristics			
Host	ha	USFS FHTET	Total area with any amount of host (pine, fir, Douglas-fir) present, per cell. Based from data collected 2002–2009
36 year average precipitation	mm	PRISM	Average annual precipitation over years 1981–2016
Cell location	Degrees	ArcMap	Latitude, Longitude
Fire history	ha	CalFire	Area burned each year per cell, 1993–2015
Bark Beetle Attack History			
Area with mortality within cell	ha	USFS FHP	Area with any amount of BB-WB-D mortality within each cell per year, from aerial surveys 1993–2016
Maximum area affected in adjacent cells	ha	USFS FHP	Area with BB-WB-D mortality from one of the eight neighboring cells that has the highest value in that category
Number of trees killed	Number	USFS FHP	Total number of newly killed trees mapped each year from 2004 – 2016 from aerial surveys per cell
Weather History			
Precipitation previous year	mm	PRISM	Total precipitation per year, between Oct 1 of previous year to Sept 31 of current year
Precipitation 2–4 years ago	mm	PRISM	Total precipitation per year, between Oct 1 to Sept 31for previous 2–4 years
Minimum winter temperature	C	PRISM	Lowest daily minimum temperature occurring from December through February of the following year

USFS FHTET – US Forest Service Forest Health Technology Enterprise Team.
USFS FHP – US Forest Service Forest Health Protection.
CalFire – http://www.fire.ca.gov/.
PRISM – PRISM Climate Group, Oregon State University.

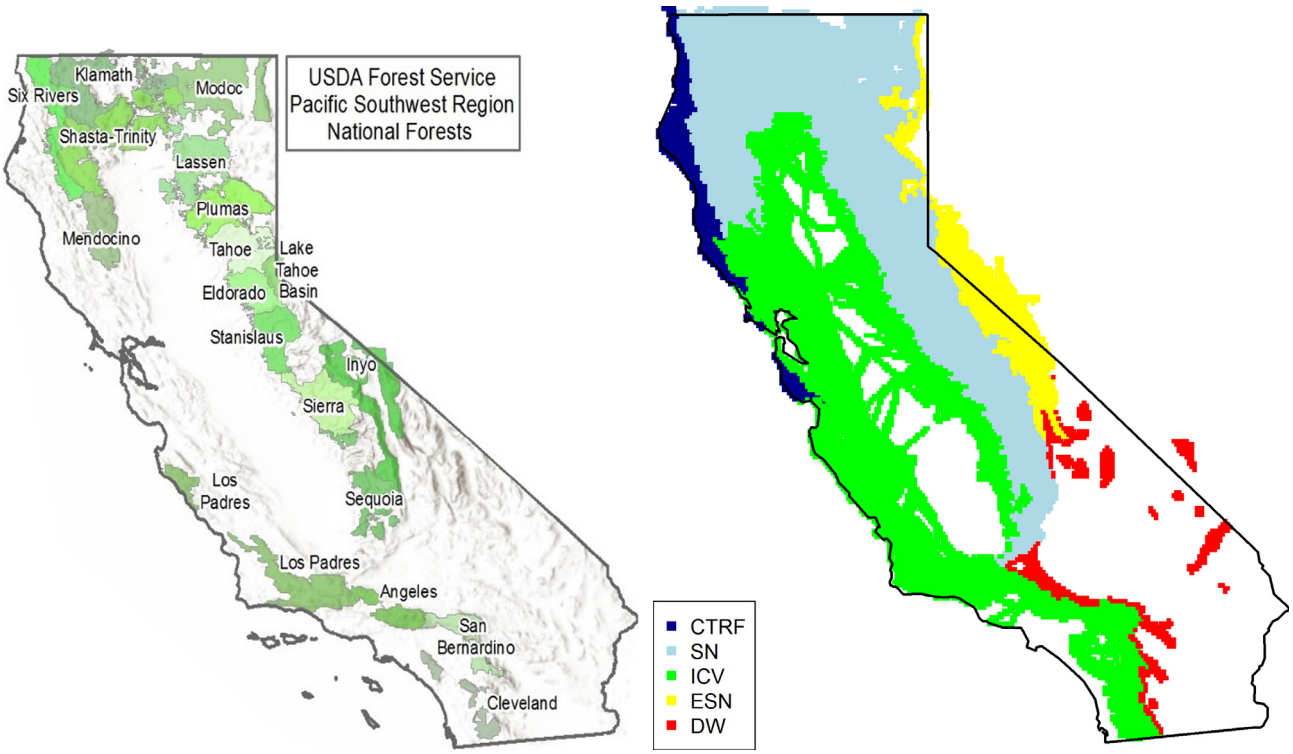

Fig. 1. (left) Map of National forests in California and (right) locations of five ecoregions: CTRF = Central temperate rain forest (4.5% of sampled cells); SN = Sierra Nevada (70%); ICV = Interior central valley (21%); ESN = Eastern Sierra Nevada (4%); DW = Desert woodland (0.5%).

Precipitation data was obtained from a modeled climate data set (PRISM; Parameter elevation Regression on Independent Slopes Model, Daly et al., 2008), also at a 2.5 min resolution, and was summed based on the hydrologic year (October 1 to the following September 30) for each year from water year 1988 to 2016. Temperature data was also sourced from PRISM. The lowest daily minimum temperature occurring from December through February of the following year was extracted from PRISM data (2.5 min resolution) for each cell from December 1991 to January 2016. Thirty-six years of average annual precipitation per pixel from 1981 to 2016 was also included as a variable (36 year average precipitation).

2.2. Ecoregions

For the purposes of our analyses, we divided California into five ecoregions, roughly based on Miles and Goudey (1997) (Fig. 1). The five ecoregions assessed here combined two to five provinces, and in some cases separated out a Section from a Province (e.g., Eastern Sierra Nevada from the Sierra Nevada). Because locational (edaphic) and environmental drivers (precipitation, precipitation, and seasonality) were included only for the pixels included in the analysis, these combinations and division are not confounded by grouping more finely defined ecoregions, or dividing provinces. The **Sierra Nevada** (**SN**) was comprised of the California chaparral forest and shrub Province (M261). The **Eastern Sierra Nevada** (**ESN**) was comprised of 341D (Mono Section) and 342B (Northwestern Basin and Range Section) (both components of the Intermountain Semi-Desert Province). The **Desert Woodlands** (**DW**) included western margins, and eastern patches of 322A (Mojave Desert Section, American Semi-Desert and Desert Province), eastern margins of M262B (southern California Mountains and Valleys Section and California Coastal Range Open Woodland-Shrub-Coniferous Forest-Meadow Province), and patches of 341F (Southern Great Basin Section, Intermountain Semi-Desert Province). The **Interior Central Valley** (**ICV**) included the coastal range M261B (Northern California Coast Ranges Section), C (Northern California Interior Coast Ranges Section), and F (Sierra Nevada Foothills Section); and M262A (Central California Coast Ranges Section), and B (Southern California Mountains and Valley Section). The M261 Sections are components of the Sierra Steppe-Mixed Forest-Coniferous Forest Province, and the M262 Sections are components of the California Coastal Range Open Woodland-Shrub-Coniferous Forest meadow Province. Flight paths across the Central Valley would not have been included in the analysis because it is agricultural and have few natural ecosystem forest trees. The **Coastal Temperate Rainforest** (**CTRF**) was wholly described by 263A (Northern California Coast Section, California Coastal Steppe, Mixed Forest, and Redwood Forest Province).

All summaries of climate, geography, and vegetation in this section are derived from Miles and Goudey (1997). The **SN** represents the greatest portion of the area analyzed (Figs. 1 and 2). The Section includes temperate to frigid parts of high mountains with granitic and andesitic substrates, characterized by mixed conifer (lodgepole, ponderosa, and Jeffrey pines; white, red, and subalpine firs; giant sequoia; western juniper; mountain hemlock; and aspen). Other sections within the SN include northern variants of these series, including the high biodiversity forests the Siskyou Mountains in northwestern California, and drier variants, western yellow pine-dominated mixed conifer forests in northeastern California. Woodland trees in **ESN** include western, mountain, and Utah juniper, white fir, Jeffrey and bristlecone pine, mountain mahogany, and aspen. Soils are derived from volcanic and mixed alluvium. **DW** is in the southern Basin and Range geomorphic province, with sedimentary, volcanic, granitic and mixed alluvial deposits. The climate is xeric, and depending on latitude and elevation, frigid to subtropical. The sparse woodland includes Utah juniper, and pinyon and bristlecone pine. In our analysis, the southern portion of DW includes scattered trees of juniper, pinyon pine,

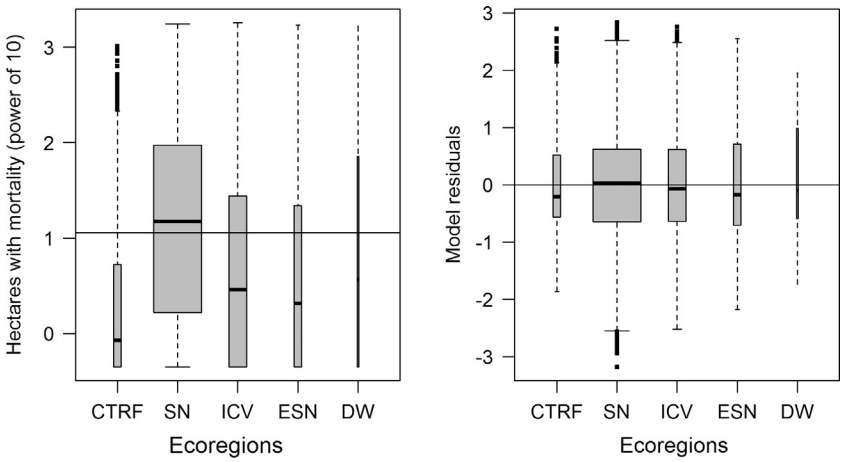

Fig. 2. (left panel) Boxplots of area with mortality per cell for each of the five ecoregions and (right panel) residuals from model after removing effects of precipitation history, BB-WB-D history and site characteristics in each of the five ecoregions. Horizontal line in each panel indicates the overall median level. The width of the boxes are proportional to the number of sampled points per ecoregion.

white fir (higher elevations), scrub live oak in uplands and northern aspects of relief, and California sycamore and Fremont cottonwood in draws with perennial sources of water in the Mojave and Colorado Deserts. Substrates are mixed. The woodlands of **ICV** are characterized by low hills, both of the coastal mountains and foothills of the Sierra Nevada. The climate has moderate temperatures and humidity, and precipitation varies with distance from the coast. The vegetation includes canyon live, Valley, coast live, California black, and blue oaks; ponderosa, Jeffrey, and lodgepole pine; incense cedar; and white fir. Substrates include sedimentary, granitic, and alluvial sources. The **CTRF** includes low mountains, hills, and valleys with sedimentary-derived substrate, and the marine influence buffering winter extremes in temperature, with cool summers and moderately high humidity year-round. Dominant vegetation includes the iconic coastal redwood, Douglas fir; white and coast live oaks, and tanoak.

2.3. Statistical model

Of concern were two dependent variables: Area per 2.5′ grid cell (1800 ha) affected by BB-WB-D mortality, and number of dead trees per 2.5′ grid cell (Table 1). Let Y_{ij} be the response variable within the ith sampled cell and year j, where a response is either area affected by mortality or number of trees killed due to BB-WB-D. We used area affected for most of our analysis because we had observations for a longer period (1993–2016) that included at least two major BB-WB-D mortality outbreaks. We used number of trees killed for producing forecasts because number of trees killed per cell is of more interest as a forecast, even though this variable was available for a shorter time period (2004–2016). The relationships between the explanatory variables and tree mortality were similar regardless of which of the two dependent variables was used. The dependent variable, Y, had a skewed distribution with values as large as 33,000 killed trees per cell (or 1800 ha affected), while more than 50% of the cells had zero mortality and 75% had less than 20 trees killed. Most parametric distributions, including extreme value distributions, did not fit our data adequately. Accordingly, we modeled the distribution of Y in two steps. In step one we used the binomial distribution to estimate $Pr[Y > \delta]$, where $\delta = 0.5$ hectares. Next we estimated the expected value of Y using only cells with Y greater than δ, $E[Y|Y > \delta]$. The unconditional expected value of Y, E(Y), is estimated by the product $Pr[Y > \delta] \times E[Y|Y > \delta]$. We used the empirical distributions of historic data to evaluate the uncertainties in our forecasts, as described below.

2.4. Model estimation

We used the following linear predictors to estimate the relationship between the explanatory variables, **X**, and the expected value of Y:

$$\text{logit}(Pr[Y_{ij} > \delta]) = \beta + \sum_{k=1}^{K} g_k(X_{kij}) + s_1(\text{long}, \text{lat}) \quad (1)$$

$$E[log_{10}(Y_{ij})|Y_{ij} > \delta] = \mu + \sum_{k=1}^{K} h_k(X_{kij}) + s_2(\text{long}, \text{lat}) \quad (2)$$

where $X_1, \ldots, X_K$ are K explanatory variables (Table 1) and the parameters $g_1, \ldots, g_K$, $h_1, \ldots, h_K$ are spline functions (Wood, 2006) describing the relationships between the explanatory variables and the response variables. The term s_j(long, lat), $j = 1, 2$, is a smooth surface of the 2.5′ cell locations (longitude, latitude) which was added to the model as a proxy for persistent features of the landscape that are not accounted for by the site characteristics already in the model. The spatially and temporally explicit explanatory variables, including the location (longitude, latitude) and size of the attacks in previous years, account for much of the spatial correlation between nearby cells. Nevertheless, some spatial correlation may still remain, especially for responses in the same year, making the standard errors produced routinely by commonly used regression programs not adequate. Therefore, we developed standard errors of the estimated parameters by fitting the models using data from all years but one. Next we repeated the process, each time leaving a different year out. Standard errors were next calculated using the Jackknife method (Preisler et al., 2012). Estimates of the functions $g_1, \ldots, g_K$, $h_1, \ldots, h_K$ from Eqs. (1) and (2) above where graphed against their corresponding explanatory variables in order to study the effect of the variables on the odds of tree mortality present (from Eq. (1)) or the effect on the mean area affected by mortality (from Eq. (2)).

2.5. Beetle pressure and weather suitability indices

The overall effect of beetle pressure and weather suitability on total tree mortality at the yearly scale was studied by estimating two indices. We used area within cell and neighboring cell affected

by mortality in the previous year as a surrogate for beetle pressure in the current year. An estimate of the total beetle pressure (Bt_{ij}) in year j was evaluated by a weighted average of the linear predictor terms, $h(X_{kij})$ from Eq. (2), corresponding to area affected in previous year, with weights, w_{ij}, given by the estimated probability that beetles are already present in the cell (from Eq. (1)). Specifically,

$$Bt_j = \sum_{iS_j} w_{ij} \times \{h(X_{1ij}) + h(X_{2ij})\}$$

where X_{1ij}, X_{2ij} are the amount of area affected by mortality within cell i and one of the eight neighboring cells with highest mortality respectively, year $j-1$, and S_j is the set of all sampled grid cells in year j (Table 1).

An estimate for the average weather suitability (WS_j) over all sampled cells in a given year was also evaluated using a weighted average of the terms in the linear predictor of equation 2 that corresponds to the amount of precipitation between Oct 1 of previous year to Sept 31 of current year and similarly for 1–4 years (Table 1). Specifically,

$$WS_j = \sum_{i \in S_j} w_{ij} \times [h(P1_{ij}) + \ldots + h(P4_{ij})]$$

where $P1, \ldots, P4$ are the amount of precipitation in grid cell i in year j. For this part of the study we used the dependent variable Y, the number of hectares affected by mortality in a given grid cell/year. This allowed us to do the analysis across a longer span of years.

2.6. Model evaluation and forecasts

We estimated the expected number of dead trees per cell in the upcoming year using the generalized additive regression models above. The number of trees killed was the dependent variable and all explanatory variables in Table 1 were used except for fire history and minimum winter temperature because these variables are not available in time to produce the forecasts in early autumn, in the year prior to the forecast. The estimated numbers were pooled into 10 Risk Levels (RL0 to RL9). With this procedure, cells that have similar site characteristics, precipitation, and mortality histories are assigned similar risk levels. In order to study goodness of fit of the forecasts, and to develop measures of uncertainties, we evaluated estimates for each year in our study by developing forecasts using information from all years but one (cross-validation). Next, we produced boxplots of the observed values for each of the ten grouped risk levels. The boxplots give an estimate of the distribution of the forecasts which can be used to assess the uncertainties around the projected values. In doing so we were able to provide an estimate of the uncertainty without resorting to parametric distributional assumptions.

3. Results

3.1. Relative contribution of ecoregions to the forecast

The greatest number of pixels contributing to the forecast was represented by the Sierra Nevada ecoregion, followed by the Interior Central Valley, the Eastern Sierra Nevada, the Desert Woodlands, and the Coastal Temperate Rainforest (Fig. 1). The area most affected by tree mortality was in the SN ecoregion (Fig. 2). However, once the precipitation history, BB-WB-D mortality history, and site characteristics were accounted for in the model, there were no significant difference in residuals among the ecoregions (Fig. 2), an indication that between-ecoregion variabilities were reasonably accounted for by the explanatory variables in the model.

3.2. Total mortality per year

The annual average area affected by BB-WB-D mortality for 1998 to 2002 was low in all regions, with an annual average of zero percent mortality per sampled cells (Fig. 3). After 2002, we note syncopated outbreaks in 2002–2006, and post 2014. In the 2002–2006 outbreaks, the southern Cascade Mountains in northern

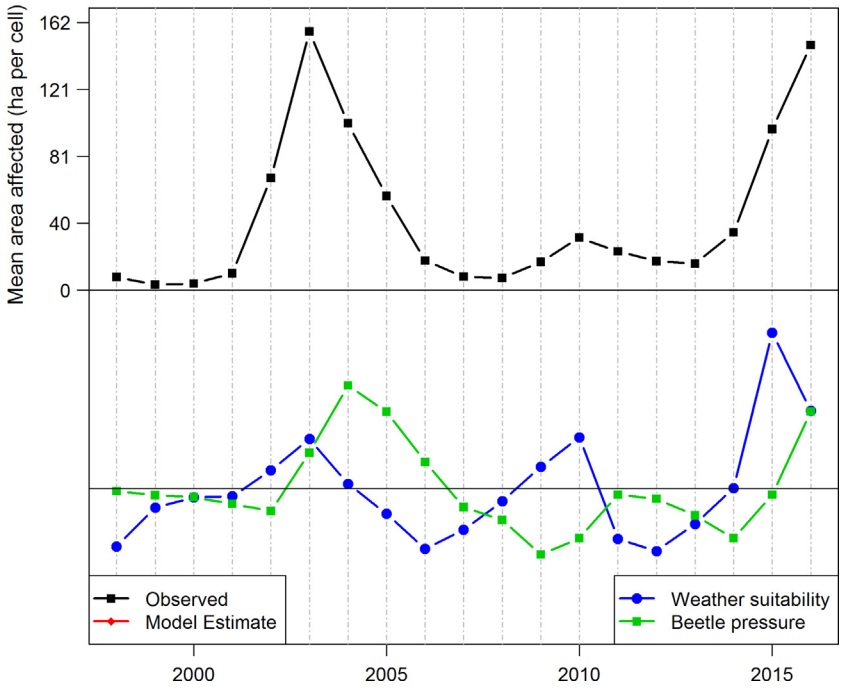

Fig. 3. Observed mean area affected (ha per 1800 ha cells) over all sampled cells in California (black). Mean area affected is highest during years where both beetle pressure (green) and weather suitability (blue) indices were above average. The weather suitability and beetle pressure indices were evaluated from the data using the regression models described in text. (For interpretation of the references to color in this figure legend, the reader is referred to the web version of this article.)

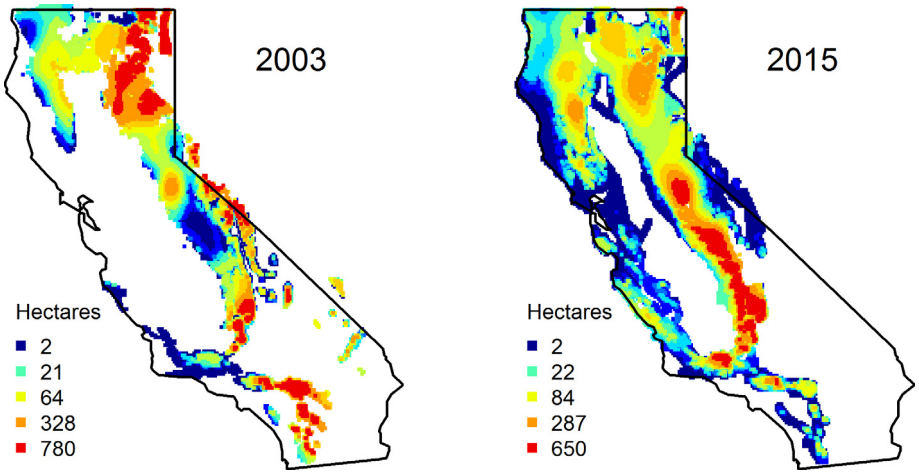

Fig. 4. Maps comparing locations with high levels of tree mortality (area affected by mortality in 2.5′ grid cells) during two major BB outbreaks in California. The first was centered round the year 2003 and the second around 2015. The legend gives the mean area affected by tree mortality in each of five colors in the map.

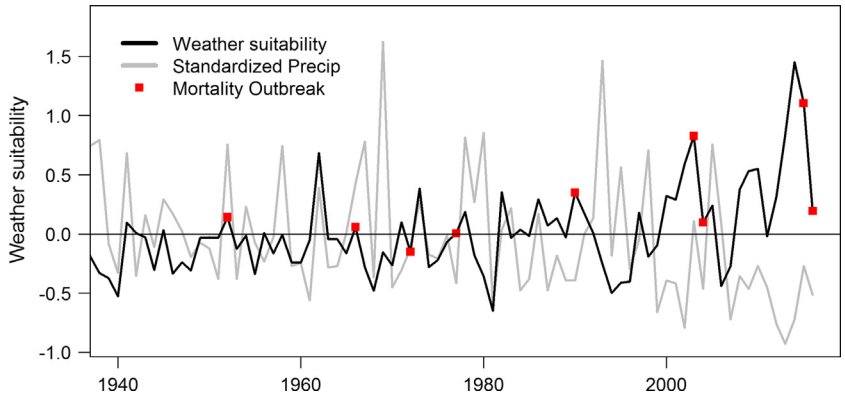

Fig. 5. Weather suitability and standardized precipitation for 129 year period in the eastern end of the San Bernardino National Forest (Big Bear Dam, San Bernardino County Water District). Almost all initial bark beetle outbreaks (red squares) occurred when weather suitability was above average but only when combined with canopy closure (Grulke et al., 2009).

California (Lassen and Plumas NF from Fig. 1), the eastern slopes of the central and southern Sierra Nevada, and the Transverse Range in southern California (San Bernardino and Cleveland NF from Fig. 1) all exhibited high levels of mortality (Fig. 4). Post-2014, high mortality was observed on the western slopes of central and south-central Sierra Nevada (Fig. 4). These outbreaks coincide with years that had both above-average 'beetle pressure' combined with above-average 'weather suitability' (Fig. 3).

The variable used to assess beetle pressure (area with mortality in the prior year), together with the variable 'remaining host,' are confounded with real time host density. The host density variable in our model is static and hence does not reflect real time density or canopy closure. However, in Grulke et al. (2009), a long term record of precipitation (129 years) in the San Bernardino Mountains, combined with aerial images from 1938 to 1998 and records of bark beetle outbreaks from the southern province entomologist to the Regional Forester (1915 to mid-1960s, and Forest Health of the USDA Forest Service records subsequently) showed that despite high weather suitability, bark beetle outbreaks did not occur until canopy closure (Fig. 5; extended from Grulke et al., 2009). In this case, canopy closure is a proxy for host density. Host density is correlated with growth (e.g., vigor), and increased tree defense against bark beetle (Kolb et al., 1998). Consequently, effects of the variables, remaining host and previous year tree mortality, reflect not only the effect of beetle pressure but also canopy closure.

3.3. Influence of site characteristics on mortality levels

The site characteristics, thirty-six year average precipitation; amount of host remaining; location (longitude, latitude); and fire, all had significant effects on both mortality and on the number of hectares affected (Table 2). For example, there were significantly higher levels of mortality at locations with large values of the 'remaining host' metric (Suppl. Fig. 1). Elevated mortality levels at locations with more remaining host is consistent with that expected. The above three spatial variables are correlated and are most likely proxies for additional spatially specific variables not already included in the model (e.g. tree density, soil moisture, or any other characteristics of a location).

The influence of the fire variable (area affected by fire per cell in previous year) on the probability of BB-WB-D mortality presence was negligible until fire extent exceeded ~1200 ha (Fig. 6a). With increases in fire extent, the probability of BB-WB-D mortality presence declined. This is partly due to the fact that trees within a fire were assumed to be killed by fire for the first two years after fire, rather than assigned to BB-WB-D related mortality. Trees with BB-WB-D mortality within a recent fire were counted only

Table 2
List of variables used in model and their effect and importance on expected number of hectares with mortality given mortality present in cell.

Variable related to	Description	Variability explained	Effect
Site characteristics		17.0%	
rhost	Remaining host = (area with host minus area with mortality prior year)	2.5%	Increasing (Supp. Fig. 1)
36 yr av precip	36 year average precipitation	3.4%	Increasing (Fig. 9)
Latitude, Longitude	Cell location	10.0%	Variable (Supp. Fig. 1)
fire	Area affected by fire 2–4 yr prior	1.0%	Increasing (Fig. 6)
Bark Beetle Attack History		12.3%	
hectare1	Area with mortality prior year	8.0%	Increasing effect starting at ~40 ha or ~2% of cell (Fig. 7)
near1	Maximum area affected in adjacent cells	4.3%	Increasing effect starting at ~125 ha or about 7% (Fig. 7)
Weather History		13.8%	
prec1	Precipitation previous year	7.6%	Increasing effect with decreasing prec1 starting ~1000 mm (Figs. 8 and 11)
prec2	Precipitation 2 yrs ago	2.5%	Increasing effect with decreasing prec2 starting ~2000 mm (Supp. Fig. 2)
prec3	Precipitation 3 yrs ago	1.0%	Increasing effect with decreasing prec3 starting ~2000 mm (Supp. Fig. 2)
prec4	Precipitation 3 yrs ago	1.7%	Decreasing effect with decreasing prec4 starting ~1000 mm (Supp. Fig. 2)
mtemp	Minimum winter temp	1.0%	Increasing with increasing mtemp starting ~−20 °C
Total of all variables		43.0%	

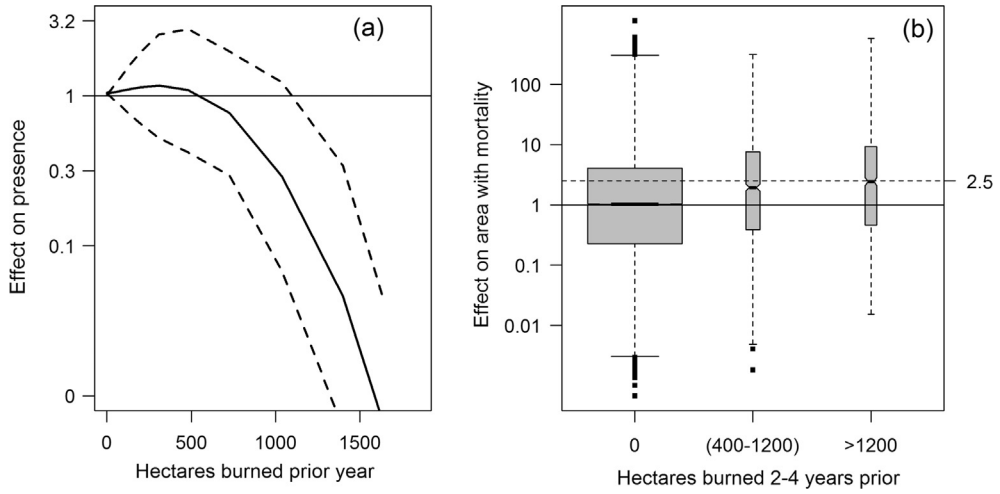

Fig. 6. (a) Estimated effects of fire history on odds of mortality presence. The y-axis is estimated odds of mortality present relative to odds at zero (i.e., no fire). (b) Partial residuals showing fold increase in total hectares with mortality in cells with mortality present, when all other variables in the model are held constant.

two-years after a fire. When tree mortality was present and fire had occurred in the past 2–4 years, the expected mortality was ~2.5-fold larger in cells with an cumulative area burned greater than 1200 ha (Fig. 6b). Ground or surface fires may damage tree roots (Preisler et al., 2000) or weaken trees (McHugh et al., 2003), which consequently increases likelihood of tree mortality.

Overall, the site characteristics accounted for ~17% of the explained variability with spatial location being the most important (Table 2).

3.4. Influence of beetle pressure on mortality levels

The area affected by tree mortality, both in a given cell and in adjacent cells in the prior year, had significant effects on the resultant area affected in the current year (Fig. 7 & Table 2). On average, the area affected was approximately 3-fold larger in cells with previous year mortality of $>10^{2.6} = 400$ ha (greater than 22% of the cell) when compared with cells with previous year mortality of $10^{1.3} = 20$ ha (less than ~1%). The effects in each of the ecoregions depended on the characteristics of the population, and the median and range of prior year tree mortality. For example, in the CTRF ecoregion, the previous year's mortality levels were mostly in the lowest mortality range, where the estimated effect is flat (Fig. 7). Only 0.4% of cells in CTRF with mortality present had previous year mortality levels of greater than 10 ha (Fig. 2). The two 'beetle pressure' variables, presence of BB in the target and adjacent cells, accounted for ~12.3% of the explained variability (Table 2).

3.5. Influence of drought on mortality levels

Annual precipitation in the previous four years had significant effect on expected area with mortality per cell, with the precipitation in the previous year being the primary driver (Table 2). We found a 10-fold increase in mortality between locations with extremely low precipitation in the previous year, when compared with locations with at least 1000 mm of rain (Fig. 8). Note, however, the non-linearity of the relationship, in that no additional significant increase or decrease is seen with increasing precipitation above

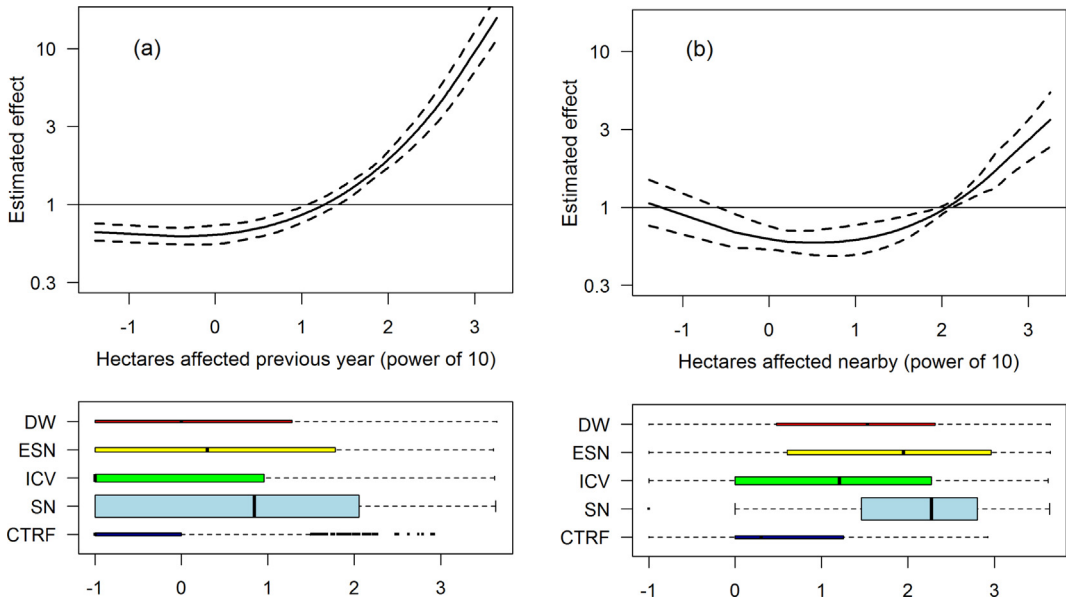

Fig. 7. Estimated effects of two beetle pressure variables on expected number of hectares affected by mortality in cells with mortality present and boxplots showing the distributions of the explanatory variables within each ecoregion. The y-axis gives the estimated fold increase in area with mortality as a function of area affected previous year when all other variables in the model are held constant.

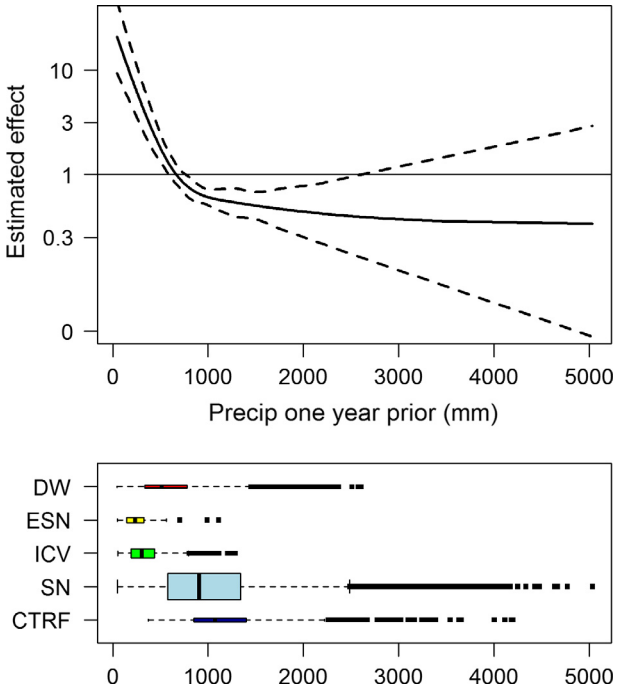

Fig. 8. Estimated effects of prior year precipitation on expected area affected by mortality in cells with mortality presence. Dashed lines are approximate point wise 95% confidence bounds. The boxplots show the range of values of the precipitation variables in each of five ecoregions. The y-axis gives the estimated fold increase in area with mortality as a function of precipitation in prior year when all other variables in the model are held constant.

1000 mm. The pattern was similar when the total precipitation two and three years prior, albeit with a smaller and less significant effects (Table 2 & Supp. Fig. 2). The effect of precipitation four-years prior on mortality levels, although only marginally significant, increased with increasing precipitation (Table 2 & Supp. Fig. 2).

In order to further explore the effects of annual precipitation relative to long term, 36-year average precipitation, on size of mortality per cell, we developed contour plots from the combined effects of these variables as estimated by the regression model in Eq. (2) (Fig. 9). First, we note an increase in expected mortality for years with prior year precipitation below the 36-year average precipitation (above the 45° line). For years with above average prior year precipitation (below the 45° line) no significant effect is observed (contour lines are mostly horizontal). Second, for the same prior year precipitation (e.g., consider a vertical line at 1000 mm) estimated effects were larger in regions with higher 36-average precipitation (wet regions) than regions with lower averages precipitation (drier regions). Drier regions (those with lower average precipitation) seem to be better buffered.

Minimum winter temperature had a marginally significant effect on area with mortality within a cell (Table 2). This variable was not used in the forecast model because of its minimal influence and because it is not available in time for the calculation of the forecasts in late autumn. Overall, the weather variables accounted for ~13.8% of the explained variability with prior year precipitation being the strongest driver in this group (Table 2).

3.6. Forecast maps

Results from combining effects of weather suitability, beetle pressure and site characteristics, via the regression models, permitted an overall risk level to be estimated for each grid cell in an upcoming year. As an example, the data from 2004 to 2016 were used to estimate risk levels for mortality in each 2.5′ cell for 2017. The risk levels where then mapped for each grid cell to produce a forecast map (Fig. 10). The map and further information about the 2017 projections can also be found at the site http://usfs.maps.arcgis.com/apps/MapJournal/index.html?appid=7b78c5c7a67748808ce298efefceaa46. Boxplots accompanying the map (Fig. 10) show the range and distribution of expected values for each of the ten risk levels, RL0 to RL9, based on ADS data from 2005–2016. We note the large amount of variability expected at each of the risk levels. The drivers, i.e. the explanatory variables, used in our model accounted for ~43% of the variability in tree mortality and appear to distinguish between cells with low risk, where 95% of the cells have zero mortality, from those with the highest risk level where

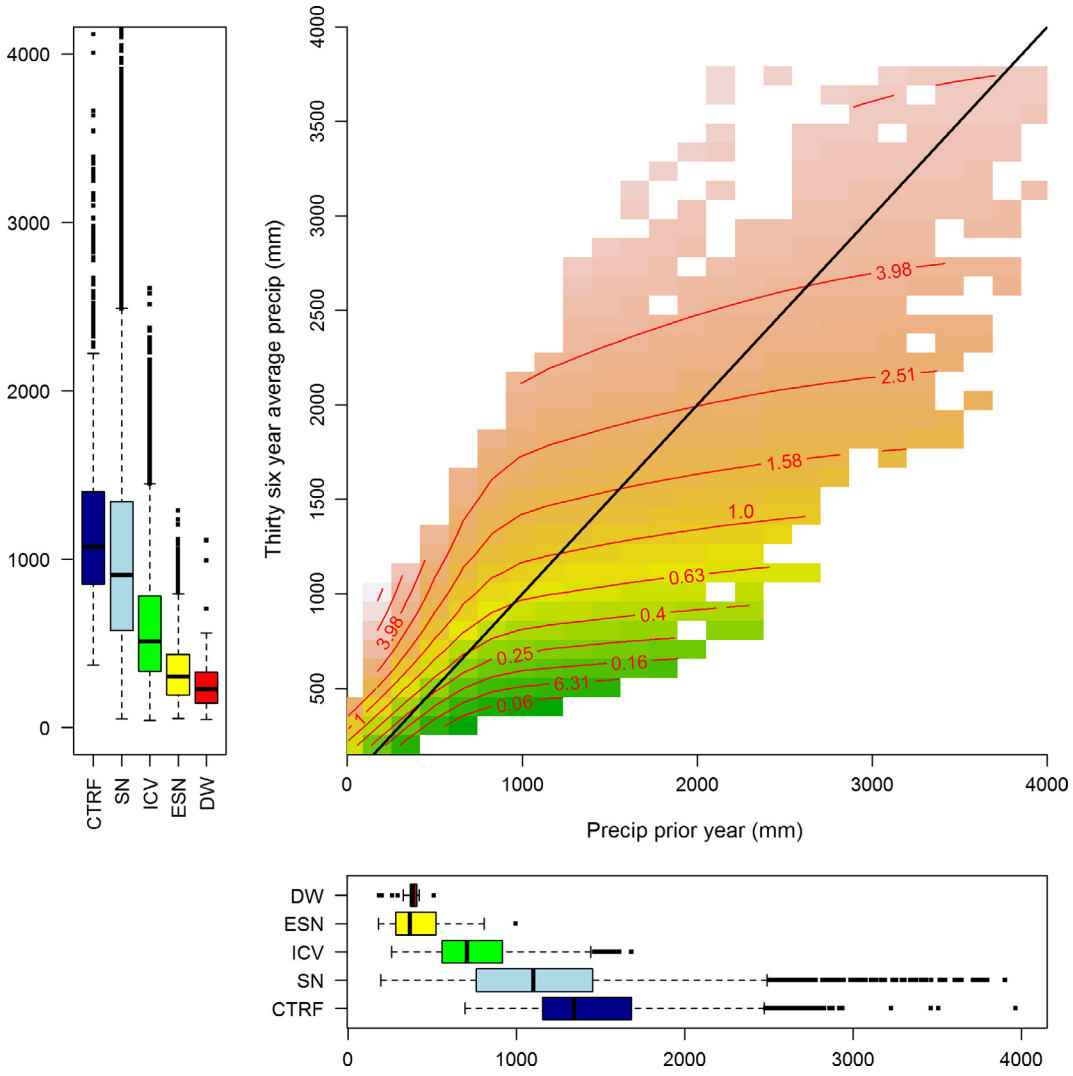

Fig. 9. Contour plots of the combined effects of 36-yrs average precipitation vs precipitation one-year prior on expected area with mortality in cells with mortality present. The 45° line separates region with above average prior year precipitation (above line) from region with below average precipitation (below line). Contour levels indicate fold increase in mortality relative to average mortality, which is set to 1. The boxplots show the range of values of the precipitation variables in each of five ecoregions.

the majority of cells have more than 10,000 trees killed per 2.5′ cell. However, there is a large overlap in the distributions of the risk levels other than the lowest and the highest levels. This demonstrates the limitation, or skill level, of our projections, in that, while we are able to distinguish between high and low risk locations, it is harder to distinguish between risk levels in the middle ranges. Outliers - cells with observed values larger than the upper 95th percentiles (Fig. 10) – especially in the lowest two risk levels, may be of concern to managers, because they indicate cases where the model failed to forecast large mortalities (albeit only in 5% or less of the cases). These are discussed in the outlier section below.

3.7. Tipping points

Our analyses suggest an estimate of what might be considered 'tipping points': when beetle pressure and weather suitability are high enough to trigger outbreaks resulting in high levels of tree mortality in upcoming years. To this end we developed bagplots (bivariate boxplots) describing the joint distribution of two of the strongest drivers, other than site characteristics, for the lowest two and highest three risk levels (Fig. 11). The bagplots show the range of values for the two drivers: (1) number dead trees detected by ADS in prior year (as a surrogate for beetle pressure and possibly canopy closure), and (2) precipitation level in the prior year (as an indication of drought). Note, almost all points at the three highest risk levels (RL7, RL8, and RL9 from Fig. 10) occurred when prior year precipitation was less than ~1000 mm (see also Fig. 8) and mortality in the prior year was greater than ~640 (=10^2.8) trees killed per cell (~4% of cell affected by mortality). The bivariate median of the bagplot for the highest risk levels was 3400 trees and 670 mm of precipitation. According to our data, when weather was suitable for mortality (precipitation prior year <1000 mm), we should expect high levels of tree mortality (>1000 trees or ~6% of cell) in the upcoming year if, additionally, beetle pressure was high (>640 dead trees or ~4% of cell). However, when the weather was not suitable (prior year precipitation >1000 mm), the percentage of a cell affected by mortality remained around 7% on average even when the beetle pressure was high (~20% of cell affected by mortality prior year). The variabilities (scatter of points) seen in the bagplots around the bivariate medians are due to other variables affecting mortality, some of which were included in the model (e.g., site characteristics) and some not included (e.g., exact number of live host trees remaining in cell).

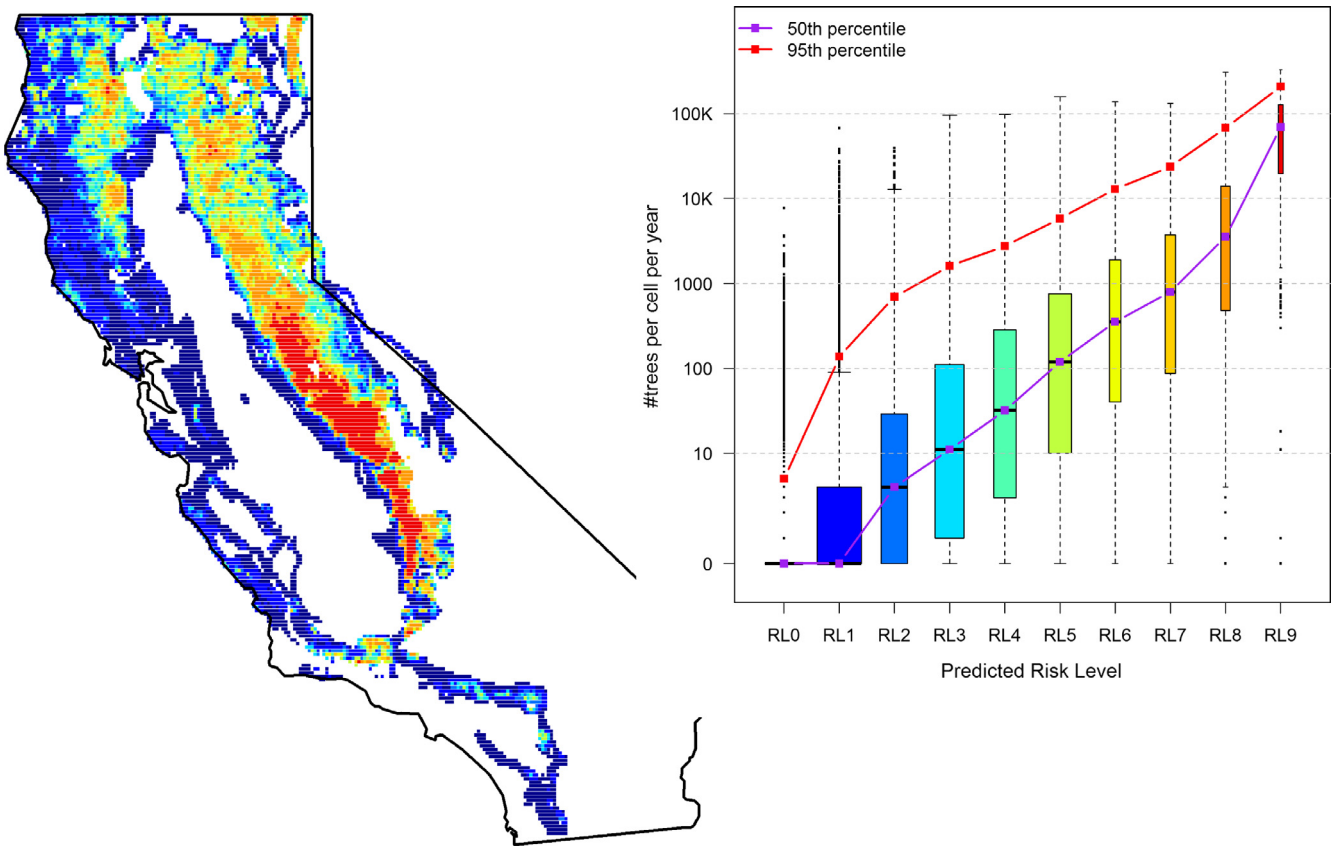

Fig. 10. Map showing projected risk level for each 2.5′ cell (1800 ha) for 2017 based on site characteristics and history of precipitation and tree mortality up to September 2016. The boxplots show the range and distribution of expected values for each of the ten risk levels (RL0–RL9) based on ADS data from 2005–2016.

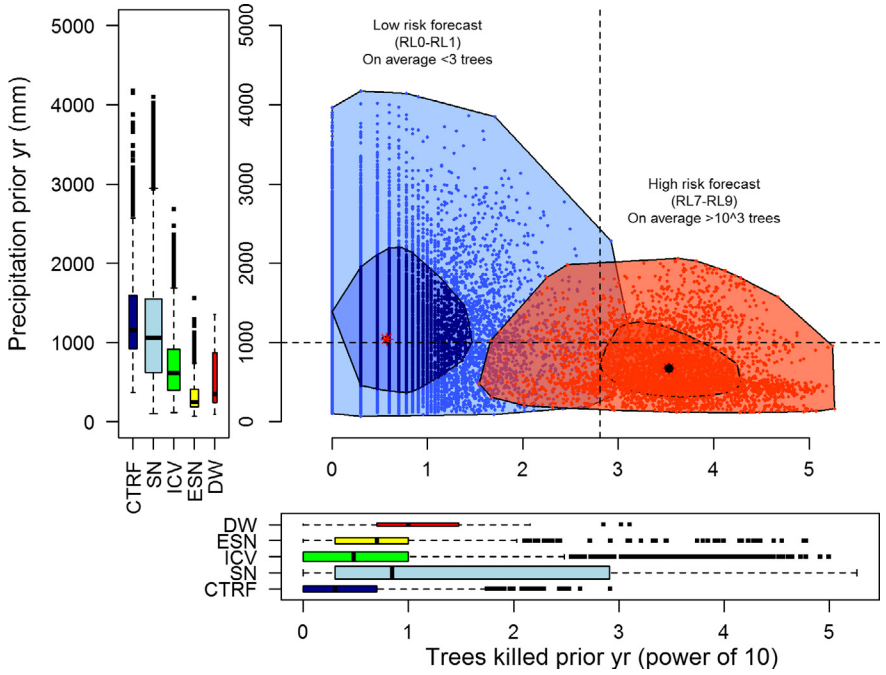

Fig. 11. Bi-variate distributions of two drivers in the forecast model: Number of trees killed prior year and precipitation level prior year, for two risk levels. The two risk groups are a combination of the lowest (RL0, RL1) and highest (RL7–RL9) risk groups in Fig. 10. The bi-variate medians (#trees, precipitation) for the two risk groups were: Low risk (3.7 trees, 1041 mm); High risk (3400 trees, 670 mm). The vertical dashed line is at 2.8 (10^2.8 = 640 trees per cell). The majority of points in the high risk group are those with previous year mortality >640 trees (~4% cell).

3.8. Outliers diagnostics maps

Outliers are cells where the projected mortality using our model was found to be significantly lower or higher than the observed values. Outliers that were particularly troublesome were those where the model predicted low or no risk of tree mortality and yet a large number of trees were recorded dead (Fig. 10). There were also a few outliers at the highest risk levels with lower than expected mortality. There may be multiple reasons for outliers, including: (1) The recorded ADS data at these locations may have been wrong, e.g., mistakes by the surveyor (due to spatial and errors of attribution); (2) An important variable may have been missing from the model that was the driver for the higher than expected mortality; (3) Depending on the timing of beetle emergence and flight, some of the mortality may have occurred after the survey; (4) Outliers could have been attributed to random error (part of the 5% error), in which case a map of their locations should be random, with no clustering of points in a given region; (5) There may have been an emerging outbreak, previously undescribed, triggered by a driver not in our model. Maps showing the locations of outliers for 2015 and 2016 projections (Supp. Fig. 3) had more outliers in the Northern California Coastal region than was expected by our model. The majority of these outliers (85%) were at locations where prior year mortality was negligible. The Coastal Temperate Rain Forest, in particular, had significant mortality in Douglas fir in recent years due to flat-headed fir borer (Pers. Comm., Bill Schaup, R6 FHP).

4. Discussion

Our annual forecast for landscape-level tree mortality in California forests and woodlands was based on weather suitability (1–4 prior year, and 36 year average precipitation), area affected by fire in each pixel with fire history in the last 1–4 years, and beetle pressure (the proportion of mortality both in the target and neighboring cells) under current conditions, i.e., high host density. Although temperature attributes (winter highest minimum; summer maximum; growing degree days) are key components in mechanistic models predicting specific insect and host demographics (e.g., mountain pine beetle on western yellow pine hosts; Régnière et al., 2012) (see FHAAST website), these metrics were not used in our forecast model because they are not available in time for the calculation of the forecasts in late autumn. Although bark beetles were likely dominant agents of insect-caused mortality especially in the Sierra Nevada, they were not the only agents contributing to tree mortality. Tree mortality due to drought was not differentiated from insect-caused mortality in ADS. Consequently, during the extreme five-year drought (2012–2016) in California, a greater proportion of mortality was likely due to physiological tree drought stress, and in many cases possibly confounded with a temperature-driven increase in insect populations.

The long term average precipitation aptly sorts the ecoregions, as they are largely defined by constituent vegetation assemblages, which are both permitted and limited by patterns and extremes in temperature and moisture regimes, as well as edaphic characteristics and resources. When environmental driving factors are outside of previously experienced extremes by the host, as in the California drought from 2012 to 2016, sensitive components of the vegetation succumb, likely proportionally to the level of stress imposed by competition (Seidl et al., 2014). These attributes are key explanatories in up-to-the-present assessments. Californian ecoregions with 36-year average precipitation above ~1000 mm were more sensitive to below average prior year annual precipitation, and had relatively greater tree mortality within a cell. Californian ecoregions with low, long-term average annual precipitation had relatively lower tree mortality than that of ecoregions acclimated to higher average annual precipitation (Fig. 9). Some of the previously published literature suggests that ecosystems with higher average precipitation may be better buffered against a single year of less-than-average precipitation than ecosystems with lower average precipitation, and that marginal populations of trees are more susceptible to extreme events (Lawton, 1993; IPCC, 2014). However, chronically stressed trees have been shown to better survive environmental stress in a northeastern US forest (McNulty et al., 2014), and in mixed conifer forests in south central Oregon (Nancy Grulke, unpublished data). The fact that ecoregions with high long term precipitation was positively correlated with greater tree mortality, after controlling for all other variables in the model, suggests that risk of tree mortality is affected by the characteristics of ecoregions, including some that are not in our models (this study and Young et al., 2017).

In 2015 and 2016, there were three areas where our projections indicated low risk of mortality and yet the observed mortality was substantially larger (Supp. Fig. 3): the Coastal Temperate Rain Forest (263A, North Coast Range Section); the Sierra Nevada (M261B, Northern California Coastal Range Section; and the extreme southern extension of the Sierra Nevada Province). Additionally, the average projected mortality per predicted risk level for August 2016 was higher than the average from all years (Fig. 12) at almost all the risk levels. In particular, average mortality at the highest (RL9) risk level for 2016 was more than 100 fold larger than the average from all years (2004–2016). Although our projections for 2016 correctly forecast high risk locations in most of the Sierra Nevada Province (M261A, Klamath Mountains Section and M261G, Modoc Plateau Section) and the forecasted numbers were within the provided variability levels, there was an intensification of mortality that produced higher than expected average numbers. Much of the difference between expected and observed tree mortality in these projected high risk areas may be explained by the unprecedented extreme drought experienced by the hosts, especially in the southern Sierra Nevada. Trees can take 3–8 years to succumb to extreme stressors (McDowell, 2011) and the biological responses can lag behind the events themselves. However, some of the mortality in area with projected low risk, especially in the Coastal Temperate Rainforest, may be attributable to flat-headed fir borer in Douglas fir (USDA Forest Service, Forest Health Protection, Region 5: Sheri Smith and Dan Cluck, *personal observation* and *communication*; Region 6: Bill Schaup *personal communication*). In the past, fir borer behaved as a minor and secondary mortality agent, but since 2015 in northwest California (and southern Oregon), it may have become a primary mortality agent. Novel mortality agents are not accounted for in either FHAAST (website) or Young et al. (2017). Such agents can be detected, field identified, and used to update the model and forecast *annually* in the present analysis. This is an important step as endemic species increase to outbreak levels, new behaviors may develop, and as new exotic insects are detected as mortality agents by ADS.

We analyzed the effect of prior 1st, 2nd, 3rd and 4th year and the average of the prior 36 years of precipitation on expected tree mortality. In the Pacific Northwest, bark beetle outbreaks were correlated with current and prior year precipitation levels (Preisler et al., 2012). In the present study, prior 1st, 2nd, 4th year, and the average 36 years of precipitation all had significant effects on expected tree mortality in August of the target year. In a case study in the San Bernardino Mountains (Grulke et al., 2009), low precipitation, and specifically a low percent of the long term average precipitation elicited moderate (< 80% of long term average) and severe (<60%) physiological drought stress. Extending this long term precipitation record through 2016, showed that over the last decade, the average precipitation was 55% of the long term (129 year) average. Throughout the 129 year record, multiple years

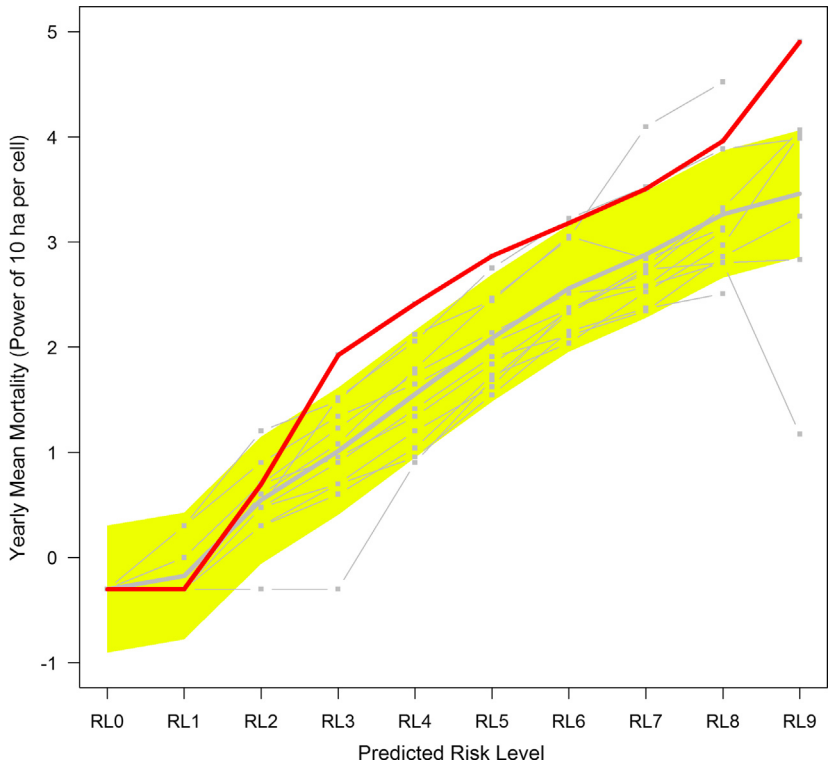

Fig. 12. Yearly mean mortality at each predicted risk level. Grey line is the mean overall years. Red line depicts the 2016 means. Yellow shows region within one standard deviation of the between year variability.

of low precipitation sufficient to elicit moderate and severe physiological drought stress was associated with initial bark beetle outbreaks in ponderosa pine (as observed by the US Forest Service, Pacific Southwest Region, Southern Province entomologists): *but only after canopy closure occurred* (Grulke et al., 2009). Stand density is an assumed correlate, and an often cited driver of tree drought stress, susceptibility to successful bark beetle attack, and subsequent tree mortality (Raffa et al., 2008 and references therein). Young et al. (2017) cited local basal area as a significant predictor of tree mortality in Californian ecoregions (one of their stand characteristics). In this paper, area with available host minus area with mortality prior year was used as a surrogate for amount of host remaining in the cell. Better metrics for remaining host trees, or density of host, may decrease the variability in our forecasts.

Beetle pressure (as indicated by area already affected by mortality) in the target and in neighboring cells was a significant correlate of expected tree mortality in the target cell (Fig. 7). Within a cell (1800 hectares), those with ~ 400 ha (22% of the area) affected by mortality in the prior year had three times greater mortality in the current year than cells with 40 ha (~2% of area) (Fig. 7a). A neighboring cell with mortality had a similar effect with a 1.8-fold increase in BB-WD-D mortality in the target cell (Fig. 7b). These effects were similar across all ecoregions, but the effect of mortality in neighboring cells were less likely to have an effect on target cell mortality in the Coastal Temperate Rainforest. Seidl et al. (2015) described the importance of stand-, local-, regional-, and landscape-level bark beetle presence in predicting tree mortality. His conclusion was that landscape-level infestations influenced beetle-caused mortality at the smallest scale (stand-level), and similar to wildfire risk, should be assessed and managed at the landscape-level.

There was a significant interaction between beetle pressure and weather suitability, as has been summarized in Anderegg et al. (2015; and references therein). Under drought conditions even low beetle pressure (4% of the cell with mortality) seemed to stimulate an increase in the area with mortality within a cell (Fig. 11). With precipitation levels >1000 mm, roughly 20% of the cell would have to be affected by BB-WB-D mortality in the prior year in order to stimulate a moderate increase in mortality (on average about 1200 trees or ~7% of cell affected).

The effect of wildfire on bark beetle outbreaks and tree mortality is complex, due to the severity (trees fully consumed or partially damaged; crown fire or surface fire) and extent of the wildfires (most or few neighboring cells have also been consumed), and the dynamics of needles, and fine, medium, and coarse branch loss (reviewed in Hicke et al., 2012). Larger wildfires may have greater fire severity (Vaillant and Reinhardt, 2017), and may also have greater patchiness of fire severity, with a greater number of trees damaged but not killed directly by the fire. In our analysis, if ~50% of the cell (~900 ha) was burned in the prior 2–4 years (Fig. 6b), the number of hectares with BB-WB-D mortality within that cell was greater on average than at location with <400 ha burned. Ground or surface fires may damage tree roots (Preisler et al., 2000) and weaken trees (McHugh et al., 2003) resulting in an increase in susceptibility of trees to drought and BB-WB attacks.

The question is often raised regarding effect of tree mortality on fire. Although not the focus of the present paper, we did have the data to consider this question (Supplement Fig. 4). According to our data, the area affected by fire was ~1.8 times larger on average in cells with tree mortality levels greater than 125 ha than cell with mortality less than 125 ha.

Our analysis was based on generalized additive models (GAM) that allowed the fitting of potentially non-linear effects of the drivers. Moreover, while GAM procedures are based on some distributional assumptions, measures of uncertainties in our forecasts where based on the empirical distribution of the data, and therefore were not bound by unwarranted assumptions. The latter is

important in studies of tree mortality at the landscape level due to the extreme skewness of the data and the lack of any parametric distribution that gives an adequate fit to the data.

Our analyses were intended to identify explanatories that could best *forecast* tree mortality using data available in the autumn before the following growing season. To be accurate (<2.5% error), the out-year forecast must be corrected annually using ADS observations, especially to detect new sources of mortality. This analysis identifies and specifies thresholds of environmental and biotic stressors, and their interactive effects that will increase expected tree mortality in a specific location for land and resource managers in the state of California. The information is provided approximately one year in advance on the project website (http://usfs.maps.arcgis.com/apps/MapJournal/index.html?appid=7b78c5c7a67748808ce298efefceaa46).

Acknowledgments

We would like to thank Fran Sapio, Frank Krist and Mark Zweifler (FHASST) and Charlie Schrader (WWETAC) for providing some of the forest health and weather data. We also like to thank Jim Ellenwood – FIA National Remote Sensing Program Manager – for developing the presence/absence host layer used in our analysis.

Appendix A. Supplementary material

Supplementary data associated with this article can be found, in the online version, at http://dx.doi.org/10.1016/j.foreco.2017.05.039.

References

Allen, C.D., Macalady, A.K., Chenchouni, H., Bachelet, D., McDowell, N., Vennetier, M., Kitzberger, T., Rigling, A., Breshears, D.D., Hogg, E.H., et al., 2010. A global overview of drought and heat-induced tree mortality reveals emerging climate change risks for forests. Forest Ecol. Manage. 259, 660–684.

Anderegg, W.R.L., Hicke, J.A., Fisher, R.A., Allen, C.D., Ankema, J., Bentz, B., Hood, S., Lichstein, J.W., Macalady, A.K., McDowell, N., Pan, Y., Raffa, K., Sala, A., Shaw, J.D., Stephenson, N.L., Tague, C., Zeppel, M., 2015. Tree mortality from drought, insects, and their interactions in a changing climate. New Phytol. 208 (3), 674–683.

Bentz, B.J., Regniere, J., Fettig, C.J., Hansen, E.M., Hayes, J.L., Hicke, J.A., Kelsey, R.G., Negron, J.F., Seybold, S.J., 2010. Climate change and bark beetles of the western United States and Canada: direct and indirect effects. Bioscience 60 (8), 602–613.

Buotte, P.C., Hickem, J.A., Preisler, H.K., Abatzoglou, J.T., Raffa, K.F., Logan, J.A., 2016. Climate influences on whitebark pine mortality from mountain pine beetle in the Greater Yellowstone Ecosystem. Ecol. Appl. 26 (8), 2505–2522.

California Forest Pest Council, 2016. Fostering Education on the Pests of California's Forests since 1951. <http://cfpc.wpengine.com/2010/03/california-past-forest-pest-condition-reports-1960-thru-1989/>.

Cudmore, T.J., Björklund, N., Carroll, A.L., Lindgren, S., 2010. Climate change and range expansion of an aggressive bark beetle: evidence of higher beetle reproduction in a naïve host tree population. J. Appl. Ecol. 47 (5), 1036–1043.

Daly, C., Halbleib, M., Smith, J.I., Gibson, W.P., Doggett, M.K., Taylor, G.H., Curtis, J., Pasteris, P.P., 2008. Physiographically sensitive mapping of climatological temperature and precipitation across the conterminous United States. Int. J. Climatol. 28, 2031–2064.

Ellenwood, J.R., Krist, F.J., Romero, S.A., 2015, National Tree Species Atlas. Fort Collins, Colorado: USDA Forest Service, Forest Health Technology Enterprise Team, FHTET-2015-01, 326 p.

Gillespie, A.J.R., 1999. Overview of the annual inventory system established by FIA. J. For. 97 (12), 16–20.

Grulke, N.E., Paine, T., Minnich, R., Chavez, D., Riggan, P., Dunn, A., 2009. Air pollution increases forest susceptibility to wildfire. In: Bytnerowicz, A., Arbaugh, M., Riebau, A., Andersen, C. (Eds.), Wildland Fires and Air Pollution. Developments in Environmental Science, vol. 8. Elsevier Publishers, The Hague, Netherlands, pp. 365–403.

Hicke, J.A., Johnson, M.C., Hayes, J.L., Preisler, H.K., 2012. Effects of bark beetle-caused tree mortality on wildfire. For. Ecol. Manage. 271, 81–90.

IPCC, 2014. Climate Change 2014: Synthesis Report. Contribution of Working Groups I, II and III to the Fifth Assessment Report of the Intergovernmental Panel on Climate Change [Core Writing Team, R.K. Pachauri and L.A. Meyer (Eds.)]. IPCC, Geneva, Switzerland, 151 pp.

Kolb, Thomas E. et al., 1998. Regulation of ponderosa pine foliar physiology and insect resistance mechanisms by basal area treatments. Tree Physiol. 18 (6), 375–381.

Krist Jr., F.J., Sapio, F., Tkacz, B.M., 2010. A multicriteria framework for producing local, regional, and national insect and disease risk maps. Advances in Threat Assessment and Their Application to Forest and Rangeland Management. USDA Forest Service, Pacific Northwest Research Station, PNW-GTR-902, pp. 621–636. <https://www.fs.fed.us/foresthealth/technology/nidrm.shtml>.

Lawton, J.H., 1993. Range, population abundance, and conservation. Trends Ecol. Evol. 8, 409–413.

McDowell, N.G., 2011. Mechanisms linking drought, hydraulics, carbon metabolism, and vegetation mortality. Plant Phys. 155 (3), 1051–1059.

McHugh, C.W., Kolb, T.E., Wilson, J.L., 2003. Bark beetle attacks on ponderosa pine following fire in northern Arizona. Environ. Entomol. 32 (3), 510–522.

McNulty, S.G., Boggs, J.L., Sun, G., 2014. The rise of the mediocre forest: why chronically stressed trees may better survive extreme episodic climate variability. New Forest. 45 (3), 401–415.

Meddens, A.J.H., Hicke, J.A., 2014. Spatial and temporal patterns of Landsat-based detection of tree mortality caused by a mountain pie beetle outbreak in Colorado, U.S.A. For. Ecol. Manage. 322, 78–88.

Miles, S.R., Goudey, C.B., (comp), 1997. Ecological sub-regions of California: Section and subsection descriptions. USDA Forest Service, Pacific Southwest Region, San Francisco, CA, R5-EM-TP-005, pp. 200.

Preisler, H.K., Haase, S.M., Sackett, S.S., 2000. Modeling and risk assessment for soil temperature beneath prescribed forest fires. Environ. Ecol. Stats. 7, 239–254.

Preisler, H.K., Hicke, J.A., Ager, A.A., Hayes, J.L., 2012. Climate and weather influences on spatial temporal patterns of mountain pine beetle populations in Washington and Oregon. Ecology 93 (11), 2421–2434.

Raffa, K.F., Aukema, B.H., Bentz, B.J., Carroll, A.L., Hicke, J.A., Turner, M.G., Romme, W.H., 2008. Cross-scale drivers of natural disturbances proneto anthropogenic amplification: the dynamics of bark beetle eruptions. Bioscience 58 (6), 501–517.

Régnière, J., Powel, J., Bentz, B., Nealis, V., 2012. Effects of temperature on development, survival and reproduction of insects: experimental design, data analysis and modeling. J. Insect Phys. 58, 634–647.

Seidl, R., Chelhass, M.-J., Rammer, W., Verkerk, P.J., 2014. Increasing forest disturbances in Europe and their impact on carbon storage. Nat. Climate Change 4 (9), 806–810.

Seidl, R., Müller, J., Hothorn, T., Bässler, C., Heurich, M., Kautz, M., 2015. Small beetle, large-scale drivers: how regional and landscape factors affect outbreaks of the European spruce bark beetle. J. Appl. Ecol. 53 (2), 530–540.

Vaillant, N.M., Reinhardt, E.D., 2017. An evaluation of the Forest Service hazardous fuels treatment program: are we treating enough to promote resilience or reduce hazard? J. For. http://dx.doi.org/10.5849/jof.16-067.

Wood, S.N., 2006. Generalized Additive Models: An Introduction with R. Chapman and Hall/CRC Press, pp. 410.

Young, D.J.N., Stevens, J.T., Earles, J.M., Moore, J., Ellis, A., Jirka, A.L., Latimer, A.M., 2017. Long-term climate and competition explain forest mortality patterns under extreme drought. Ecol. Lett. 20, 78–86.